Published in final edited form as:
Immunity. 2009 September 18; 31(3): 513–525. doi:10.1016/j.immuni.2009.08.010.

Origin of the Lamina Propria Dendritic Cell Network

Milena Bogunovic[1,2], **Florent Ginhoux**[1,2], **Julie Helft**[1,2], **Limin Shang**[2], **Daigo Hashimoto**[1,2], **Melanie Greter**[1,2], **Kang Liu**[3], **Claudia Jakubzick**[1,2], **Molly A. Ingersoll**[1,2], **Marylene Leboeuf**[1,2], **E. Richard Stanley**[4], **Michel Nussenzweig**[3,5], **Sergio A. Lira**[2], **Gwendalyn Randolph**[1,2], and **Miriam Merad**[1,2,*]

[1]Department of Gene and Cell Medicine, Mount Sinai School of Medicine, 1425 Madison Ave., New York, NY 10029, USA.

[2]Immunology Institute, Mount Sinai School of Medicine, 1425 Madison Ave., New York, NY 10029, USA.

[3]Laboratory of Molecular Immunology, The Rockefeller University, New York, New York 10065, USA.

[4]Department of Developmental and Molecular Biology, Albert Einstein College of Medicine, 1300 Morris Park Ave., Bronx, NY 10461, USA.

[5]Howard Hughes Medical Institute, The Rockefeller University, New York, New York 10065, USA.

Abstract

CX3CR1$^+$ and CD103$^+$ dendritic cells (DCs) in intestinal lamina propria (LP) play a key role in mucosal immunity. However, the origin and the developmental pathways that regulate their differentiation in the LP remain unclear. Our results reveal that monocytes give rise exclusively to CX3CR1$^+$CD103$^-$ LP DCs under the control of M-CSFR and Flt3 ligands. In contrast, common DC progenitors (CDP) and pre-DCs, which give rise to lymphoid organ DCs but not to monocytes, differentiate exclusively into CD103$^+$CX3CR1$^-$ LP DCs under the control of Flt3 ligand and GM-CSF. CD103$^+$CX3CR1$^-$ DCs but not CX3CR1$^+$CD103$^-$ DCs in the LP constitutively express CCR7 and are the first DCs to transport pathogenic *Salmonella* from the intestinal tract to the mesenteric lymph nodes. Altogether, these results underline the diverse origin of the LP DC network and identify mucosal DCs that arise from pre-DC as key sentinels of the gut immune system.

Introduction

Under physiological conditions, the intestinal immune system is tolerant to food antigens as well as to commensal bacteria, whereas potent effector immune responses are induced to pathogenic microbes. How the discrimination between commensal and pathogenic bacteria occurs is unclear, but several studies suggest that mucosal dendritic cells (DCs) play a central role in this process.

DCs are present throughout the intestine where they reside in the lamina propria facing the lumen (Coombes and Powrie, 2008; Johansson and Kelsall, 2005) and in the muscular layers

*Corresponding author: Miriam Merad, 1425 Madison Avenue, New York, NY 10029. Tel: 212-659-8276. Miriam.Merad@mssm.edu.

and the serosa facing the peritoneum (Flores-Langarica et al., 2005). DCs also accumulate in intestinal lymphoid tissues that include the PP (PP) and isolated lymphoid follicles and in the mesenteric lymph nodes (MLN) (Johansson and Kelsall, 2005).

Although the phenotype of DCs in the PP has been documented, the diversity of the lamina propria DCs is only starting to be unraveled. A subset of lamina propria DCs expressing the integrin αEβ7 (also called CD103) (Cepek et al., 1994) have a superior ability to induce the expression of gut homing molecules on T lymphocytes and to drive the peripheral generation of $Foxp3^+$ T regulatory cells (Jaensson et al., 2008; Johansson-Lindbom et al., 2005; Sung et al., 2006). $CD103^+$ DCs with similar functions were also described in the MLN and were recently shown to represent the main MLN DC population to present oral antigens to T lymphocytes suggesting that they originate from the lamina propria (Coombes et al., 2007; Jaensson et al., 2008; Johansson-Lindbom et al., 2005). Consistent with this hypothesis a study in the rat identified migratory $CD103^+$ DCs in the intestinal lymph in the steady state (Huang et al., 2000). DCs that constitutively migrate to the MLN deliver antigens from both commensal bacteria (Macpherson and Uhr, 2004) and apoptotic epithelial cells (Huang et al., 2000). Impairment of constitutive DC trafficking to the MLN in mice lacking CCR7 results in defective induction of tolerance to oral antigens (Worbs et al., 2006) establishing the importance of constitutive antigen transport to the MLN in mucosal integrity.

Another subset of lamina propria DCs characterized by the expression of the fractalkin receptor CX3CR1 plays a key role in the sampling of luminal antigens. The exact mechanisms by which lamina propria DCs sample gut antigens that are transported to the MLN continue to be an active area of investigation. Several studies established that lamina propria DCs in mice and humans sample antigens directly from the intestinal lumen by projecting dendrites through the epithelial cell layer and into the lumen (Chieppa et al., 2006; Niess et al., 2005; Rescigno et al., 2001b). The ability of lamina propria DCs to penetrate the epithelium is thought to provide a mechanism by which apoptotic epithelial cells (Rescigno et al., 2001b) and commensal organisms (Niess et al., 2005) could be captured and transported to the MLN. The formation of DC transepithelial projections in the mouse lumen has been shown to be dependent on CX3CR1 (Niess et al., 2005). Consistently, non-pathogenic *Escherichia coli* was absent from the MLN of mice that lack CX3CR1(Niess et al., 2005). However, the exact relationship between the $CX3CR1^+$ DCs specialized in the sampling of intestinal antigens and the tissue migratory $CD103^+$ DCs is unclear.

Recent studies characterized DC lineage commitment in the bone marrow (BM). Lymphoid tissue DCs, plasmacytoid DCs, and monocytes share a common progenitor called the macrophage and DC precursor (MDP) identified in the BM as $lineage^-CD117^{hi}$ $CX3CR1^+CD115^+$ cells (Fogg et al., 2006), whereas a distinct progenitor called the common DC precursor (CDP) ($Lin^-CD117^{lo}CD115^+$ $CD135^+$) arises from MDP (Liu et al., 2009) and is restricted to producing lymphoid organ DCs and plasmacytoid DCs (Naik et al., 2007; Onai et al., 2007c). CDP also produce pre-cDCs, a cDC restricted progenitor that has lost plasmacytoid DC differentiation potential (Liu et al., 2009). Pre-cDCs circulate through the blood to localize in lymphoid organs where they give rise to spleen and lymph nodes DCs (Liu et al., 2009). Circulating monocytes are an excellent source to generate DCs *in vitro* but their contribution to DC homeostasis *in vivo* is still unclear. Monocytes do not give rise to lymphoid organ DCs *in vivo* in the steady state but this can occur during inflammation (Naik et al., 2006). In contrast, one subset of monocytes ($Ly6C^{lo}$ $CX3CR1^{hi}CCR2^-$) has been shown to contribute to DC homeostasis in the intestine in the non-inflamed setting (Varol et al., 2007). Consistent with this hypothesis, a study in the rat has shown that $CX3CR1^{hi}CCR2^-$ monocytes give rise to tissue migratory DCs suggesting that monocytes could contribute to the $CD103^+$ lamina propria DCs (Yrlid et al., 2006). These studies lead to the hypothesis that monocytes represent a major contributor of the intestinal DC pool in the steady state.

However, the exact contribution of each of these precursors to DC homeostasis in the lamina propria remains unclear. It also remains unclear whether the two prominent lamina propria DC subsets derive from a similar precursor and represent different stages of DC differentiation or whether they represent two developmentally distinct DC subsets. Here we used adoptive transfer experiments and *in vivo* labeling studies to trace the origin of the lamina propria DC network. Our results establish that mucosal $CD103^+CX3CR1^-$ DCs and $CD103^-$ $CX3CR1^+$ DCs derive from two distinct DC lineages to serve separate immune function in the intestine.

Results

Phenotype of the gut DC network

To examine the phenotype of the DC subsets that populate different compartments of the small bowel (SB), we isolated the intestinal epithelial cell (IEC) fraction, the lamina propria depleted of PP, the muscularis together with the serosa and the PP. Cell suspensions obtained from each tissue compartment were analyzed separately by flow cytometry. We found that MHC Class II (MHC II)$^+$ $CD11c^{hi}$ DCs accumulate mainly in the IEC fraction and lamina propria and are absent from the muscularis and the serosa. Mucosal $CD11c^{hi}$ DCs can be further divided into two phenotypically distinct DC populations characterized as MHC $II^{hi}CD11c^{hi}CD103^+CD11b^+$ and $MHCII^{hi}CD11c^{hi}CD103^-CD11b^+$ DCs (Fig. 1A–B). A minor DC population characterized as $MHCII^{hi}CD11c^{hi}CD103^+CD11b^-$ DCs was also detected in the lamina propria (Fig. 1A–B). Due to the inability to fully eliminate lymphoid aggregates from the lamina propria, we asked whether the $CD103^+CD11b^-$ DCs in the lamina propria are mainly the result of lymphoid tissue contamination. Consistent with this hypothesis we found that (i) $CD103^+CD11b^-$ DCs are enriched in PP, while they are absent in the IEC fraction (Fig. 1A), (ii) $CD103^+CD11b^-$ DCs are strongly reduced in mice deficient in the inhibitor of DNA binding protein 2 (Id2) that also lack PP, while $CD103^+CD11b^+$ DCs and $CD103^-CD11b^+$ DCs remain unaffected in these mice (Fig. 1C). (iii) similar to $CD103^+CD11b^-$ DCs in peripheral lymphoid organs (not shown), mucosal $CD103^+CD11b^-$ DCs also express CD8α antigen, while CD8α is either not expressed or expressed at low levels by $CD103^+CD11b^+$ DCs and $CD103^-CD11b^+$ lamina propria DCs (Fig. 1D) . Altogether, these results suggest that the majority of $CD103^+CD11b^-$ DCs in the SB accumulates in the lymphoid tissue rather than in the lamina propria . Immunofluorescence studies of SB frozen sections reveal the presence of $CD103^+CD11c^+$ DCs in the lamina propria and in the intra-epithelial space of apical villi, while $CD103^-CD11b^+$ DCs accumulate mainly in the lamina propria (Fig. 1B; Fig. S1A–B).

CX3CR1 was expressed only by $CD103^-CD11b^+$ DCs and was absent from $CD103^+$ DCs (Fig. 1D). Using a reporter mouse expressing eGFP under the macrophage colony stimulating factor receptor (M-CSFR), we found that $CD103^+CD11b^+$ DCs expressed much lower M-CSFR transcripts levels compared to $CD103^-$ $CD11b^+$ DCs (Fig. 1D). We further established that the macrophage marker F4/80 was expressed at higher levels on $CD103^-CD11b^+$ DCs compared to $CD103^+CD11b^-$ DCs (Fig. 1D). Giemsa staining revealed that, in contrast to $CD103^+CD11b^+$ DCs, $CD103^-CD11b^+$ DCs present a vacuolar cytoplasm resembling that of macrophages (Fig. 1E). $CD103^+CD11b^+$ and $CD103^-CD11b^+$ lamina propria DCs loaded with ovalbumin peptides were both efficient at priming naïve ovalbumin-specific TCR transgenic $CD4^+$ T cells establishing their antigen presenting function (Fig. 1F). In contrast to the mucosa, the serosa and muscularis layer contained only one homogeneous DC population characterized as $MHCII^{hi}CD11c^{lo}CD103^-CD11b^+$ cells that also expressed CX3CR1 and the macrophage markers F4/80 and M-CSFR (Fig. 1A,D; Fig. S1C).

Altogether these data show that the lamina propria contains two DC populations that include $MHCII^+CD11c^{hi}CD103^+CD11b^+CX3CR1^-M\text{-}CSFR^{lo}$ DCs (referred to as $CD103^+CD11b^+$ DCs) and $MHCII^{hi}CD11c^{hi}CD103^-CD11b^+CX3CR1^+M\text{-}CSFR^{hi}$ DCs (referred to as

$CD103^{-}CD11b^{+}$ DCs), while $MHCII^{hi}CD11c^{hi}CD103^{+}CD11b^{-}CX3CR1^{-}$DCs (refereed to as $CD103^{+}CD11b^{-}$ DCs) accumulate mainly in the PP. $MHCII^{hi}CD11c^{lo}CD103^{-}CD11b^{+}$ DCs are distributed in the muscular and serosal layers of the gut distant from the lumen. Equivalent DC subsets have been found in the large bowel (not shown). The rest of the study will focus mainly on identifying the mechanisms that regulate the development of the $CD103^{+}CD11b^{+}$ and $CD103^{-}CD11b^{+}$ lamina propria DCs.

The role of growth factors in the development of lamina propria DCs

Fms like thyrosine kinase 3 (Flt3) ligand and granulocyte macrophage colony stimulating factor (GM-CSF) are two major cytokines in DC development (Merad and Manz, 2009). Flt3 ligand is a key molecule for the development of lymphoid organ DCs and mice that lack Flt3 or its ligand have a strong reduction of DCs in lymphoid organs (Onai et al., 2007b). GM-CSF is a key cytokine to generate DCs in vitro, in mice and humans (Banchereau and Steinman, 1998) but lymphoid organ DCs develop normally in mice that lack GM-CSF and GM-CSF receptor (GM-CSFR) (Vremec et al., 1997). M-CSFR ligands play a predominant role in macrophage development (Pixley and Stanley, 2004) but are also required for the development of epidermal Langerhans cells (Ginhoux et al., 2006). However, the exact role of these cytokines in the development of intestinal DCs has not been clearly established. Consistent with the different M-CSFR expression levels between the two lamina propria DC subsets, M-CSFR deletion dramatically affected the development of $CD103^{-}CD11b^{+}$ lamina propria DCs, while it did not affect the development of $CD103^{+}CD11b^{+}$ lamina propria DCs (Fig. 2A–B; Fig. S2A). In contrast, in mice that lack Flt3 or its ligand, the development of $CD103^{+}CD11b^{+}$ lamina propria DCs was strongly impaired, while $CD103^{-}CD11b^{+}$ DCs were only slightly reduced in these mice (Fig. 2A–B; Fig. S2A). Absence of GM-CSFR affected mostly the development of $CD103^{+}CD11b^{+}$ lamina propria DCs, while $CD103^{-}CD11b^{+}$ lamina propria DCs were not affected (Fig. 2A–B; Fig. S2A). Circulating monocytes were also affected in mice that lack M-CSFR or GM-CSFR but were not affected in mice that lack Flt3 (Fig. S2B)

To test whether the requirement for each cytokine receptor was intrinsic to the DC precursors, we reconstituted and lethally irradiated wild type recipient mice with a 1:1 mixture of wild type and mutant progenitors lacking specific cytokine receptors, except for the M-CSFR chimeric mice where a 1:10 mixture of wild type and $M\text{-}CSFR^{-/-}$ progenitors was used to ensure the engraftment of $M\text{-}CSFR^{-/-}$ progenitors. Consistent with the defects observed in the knock-out mice, we found that M-CSFR was required for the development of $CD103^{-}CD11b^{+}$ DCs but not for the development of $CD103^{+}CD11b^{+}$ lamina propria DCs (Fig. 2C). Flt3 was required for the development of the two lamina propria DC subsets with a stronger requirement for $CD103^{+}CD11b^{+}$ lamina propria DCs compared to $CD103^{-}CD11b^{+}$ lamina propria DCs (Fig. 2C). GM-CSFR was required for the development of $CD103^{+}CD11b^{+}$ DCs, while GM-CSFR was dispensable for the development of $CD103^{-}$ $CD11b^{+}$ lamina propria DCs (Fig. 2C). Interestingly, $MCSFR^{-/-}$ progenitors failed to give rise to $Gr\text{-}1^{lo}$ but not to $Gr\text{-}1^{hi}$ blood monocytes while $Flt3^{-/-}$ and $GM\text{-}CSFR^{-/-}$ progenitors gave rise to monocytes comparable in numbers to the wild type (Fig. S2C). These results suggest that the monocyte defect observed in GM-CSFR deficient mice was not intrinsic to the DC precursors.

The dual origin of the lamina propria DC network

To examine whether different cytokine requirements among lamina propria DCs reflected their different origin, we sought to identify the specific hematopoietic progenitor that gives rise to each specific DC population in the lamina propria. We injected purified MDP, CDP, pre-DCs and monocytes into untreated congenic mice and seven days later we measured their capacity to differentiate into intestinal DCs. In this assay, MDP gave rise to all mucosal DC subsets including $CD103^{+}CD11b^{+}$ and $CD103^{-}CD11b^{+}$ lamina propria DCs and to $CD103^{+}CD11b^{-}$

PP DCs (Fig. 3A). CDP gave rise to $CD103^+CD11b^-$ PP DCs and $CD103^+CD11b^+$ lamina propria DCs but not to $CD103^-CD11b^+$ lamina propria DCs (Fig. 3A). Consistently, pre-DCs that derive from CDP gave rise to $CD103^+CD11b^-$ DCs and to $CD103^+CD11b^+$ DCs but not to $CD103^-CD11b^+$ DCs. These results establish that in addition to giving rise to lymphoid organ DCs, pre-DCs also give rise to $CD103^+CD11b^-$ lamina propria DCs as well as to $CD103^+CD11b^-$ PP DCs.

MDP contribution to $CD103^+$ lamina propria DCs was always greater than its contribution to $CD103^-$ lamina propria DCs (Fig. 3A). These results may either reflect MDP intrinsic potential to preferentially differentiate into $CD103^+$ DCs or only reflect the higher turnover rate of $CD103^+$ DCs, which increases the probability of these cells to be replaced by blood precursors (Jaensson et al., 2008). To address this question we examined the steady state turnover of lamina propria and PP DCs using parabiotic mice. Parabiotic mice share blood circulation but have separated organs for extended period of time, providing a useful model to trace the physiological turnover of blood-derived cells. Two weeks after parabiosis was established we found that the % of donor parabiont-derived DCs was higher among $CD103^+$ lamina propria DCs compared to $CD103^-CD11b^+$ lamina propria DCs (Fig. 3B). These results suggest that $CD103^+CD11b^-$ PP DCs and $CD103^+CD11b^+$ lamina propria DCs have a higher probability to be replaced by short-lived adoptively transferred blood precursors than $CD103^-CD11b^+$ lamina propria DCs. CDP did not give rise to $CD103^-CD11b^+$ lamina propria DCs in this assay which, again, may reflect the slow turnover rate of these cells (Fig. 3B) or suggest that MDP contribution to $CD103^-CD11b^+$ DCs is mainly provided by monocytes. However, no monocyte-derived DCs were recovered in the lamina propria upon monocyte adoptive transfer experiments in the steady state (Fig. 3A).

Since MDP have a greater proliferation potential than monocytes and CDP, their potential to give rise to lamina propria DCs with longer half-life will always be higher than that of its downstream progenitors.

To address this caveat, we adoptively transferred MDP, CDP, pre-DCs or monocytes into recipient mice depleted of lamina propria DCs. To eliminate lamina propria DCs, we used transgenic mice expressing diphtheria toxin receptor (DTR) under the CD11c promoter (CD11c-DTR mice) and injected them with diphtheria toxin (DT) prior to adoptive cell transfer, as DT administration in CD11c-DTR mice was shown to deplete most tissue DCs *in vivo* (Jung et al., 2002; Varol et al., 2007). Similar to naïve mice, in DT treated mice, MDP differentiated into all lamina propria DC populations, while CDP and pre-DCs contributed mainly to $CD103^+CD11b^-$ PP DCs and $CD103^+CD11b^+$ lamina propria DCs (Fig. 3C). In contrast to the results observed in naïve mice, Gr^{hi} monocytes gave rise to lamina propria DCs in DT treated mice. Importantly, $Gr1^{hi}$ monocytes contributed mainly to $CD103^-CD11b^+$ lamina propria DC subset while they did not give rise to $CD103^+CD11b^-$ PP DCs or $CD103^+CD11b^+$ lamina propria DCs (Fig. 3C). These results suggest that CDP and pre-DCs do not significantly contribute to the $CD103^-CD11b^+$ lamina propria DC pool in the steady state gut, or even under conditions of DC depletion while monocytes differentiate mainly into $CD103^-CD11b^+$ lamina propria DCs.

Monocytes do not give rise to $CD103^+CD11b^+$ lamina propria DCs in the steady state

Our results showing that adoptively transferred monocytes give rise only to $CD103^-CD11b^+$ lamina propria DCs in DC depleted mice may be due to the slow turnover of $CD103^-CD11b^+$ lamina propria DCs as suggested by the parabiotic mouse data (Fig. 3B). Another possibility is that DT influences monocyte/DC differentiation by inducing a favorable tissue inflammatory milieu. To address this caveat, we sought to trace genetically labeled monocytes *in vivo* using the *LysM-Cre* × *Rosa26-floxstopfloxEGFP* mice (Jakubzick et al., 2008). In these mice, *Cre* activity removes a stop cassette upstream of the floxed reporter and

induces irreversible expression of eGFP in $LysM^+$ cells and their progeny. While all monocytes express LysM, not all monocytes are $eGFP^+$ in these mice (Jakubzick et al., 2008). We reasoned that DC populations expressing a much lower fraction of eGFP than blood monocytes could not be derived primarily from monocytes. Our results show that $CD103^-CD11b^+$ lamina propria DCs have eGFP levels compatible with the monocyte origin (Fig. 3D). Consistent with the results above, $CD103^+CD11b^+$ lamina propria DCs express much lower eGFP levels compared to monocytes further establishing that they do not primarily derive from monocytes in the steady state (Fig. 3D).

Lamina propria DC populations have different migratory abilities in the steady state

Tissue draining LN contain tissue migratory and resident DCs (Banchereau and Steinman, 1998). CCR7 controls DC migration from the tissue to the draining LN (Forster et al., 1999; Ohl et al., 2004) and specific DC defects in the draining LN of $CCR7^{-/-}$ mice have been used to distinguish tissue migratory DCs from LN resident DCs in the steady state. $CD103^+$ DCs are reduced in the MLN in the absence of CCR7 (Johansson-Lindbom et al., 2005). However, it is unclear in this published study whether $CD103^+CD11b^+$ lamina propria DCs are specifically affected in CCR7 deficient mice. It is also unclear whether $CD103^-CD11b^+$ lamina propria DCs are affected in these mice.

To compare the constitutive migratory ability of lamina propria DC subsets, we examined the phenotype of MLN DCs in a naïve mouse. $CD103^+CD11b^+$ DCs phenotypically identical to those present in the intestinal mucosa (not shown) were also present in the MLN (Fig. 4A). In contrast to $CD103^-CD11b^+$ lamina propria DCs, $CD103^-CD11b^+$ DCs in the quiescent MLN expressed much lower CX3CR1 levels (Fig. 4A) suggesting that $CD103^-CD11b^+CX3CR1^+$ lamina propria DCs either do not migrate to the MLN in the steady state or that CX3CR1 expression is down-regulated during DC migration. To address this caveat, we used *LysM-Cre* × *Rosa26-floxstopfloxEGFP* mice to trace the migration of genetically labeled lamina propria DCs to the draining LN (Jakubzick et al., 2008). We found that 90% of $CD103^-CD11b^+$ lamina propria DCs are $eGFP^+$, while the eGFP expression among each MLN DC subset did not exceed 20% (Fig. 4B). Since eGFP expression is irreversible in these mice, these results establish that $CD103^-CD11b^+CX3CR1^+$ lamina propria DCs are unlikely to migrate to the MLN in the steady state. Consistent with these results, CCR7 was expressed at much higher levels in $CD103^+CD11b^+$ lamina propria DCs compared to $CD103^-CD11b^+$ lamina propria DCs (Fig. 4C). Moreover, $CD103^+CD11b^+$ DCs were strongly reduced in the MLN of $CCR7^{-/-}$ mice in the steady state, while $CD103^-CD11b^+$ MLN DCs remained unaffected in these mice (Fig. 4D, 4E). The distribution of lamina propria DCs in $CCR7^{-/-}$ mice was also not affected (not shown). Altogether these results suggest that the $CD103^+CD11b^+$ DC subset represents the main migratory DC population in the lamina propria in the steady state.

$CD103^+CD11b^+$ lamina propria DCs are specialized in the early transport of pathogens from the intestinal tract to the MLN

The striking differential CCR7 expression among lamina propria DCs prompted us to examine the differential role of the lamina propria DC populations in the early transport of pathogens from the intestinal tract to the MLN upon oral infection. To address this question, streptomycin pre-treated mice were orally infected with wild type *Salmonella* Typhimurium to enforce *Salmonella* invasion through the lamina propria, providing a clinically relevant mouse model of salmonellosis (Barthel et al., 2003). We found that 24 h after oral infection, $CD103^+CD11b^+$ DCs were the only DCs in the MLN that carried intracellular *Salmonella* (Fig. 5A–C) even though both $CD103^+CD11b^+$ and $CD103^-CD11b^+$ DC subsets contained intracellular *Salmonella* in the lamina propria at this time point (Fig. 5D–E). In contrast, after systemic infection, all DC subsets in the MLN contained *Salmonella* antigen (Fig. 5A).

Consistent with previous studies, *Salmonella* carrying cells were not detected among MLN and mucosal $CD103^+CD11b^-$ DCs of orally infected mice, suggesting that in this model *Salmonella* invades mainly through the lamina propria and not PP (Barthel et al., 2003).

The transport of *Salmonella* from the intestinal tract to the MLN is impaired in the absence of mucosal $CD103^+CD11b^+$ DCs

To examine whether the absence of $CD103^+CD11b^+$ lamina propria DCs affects the transport of intestinal pathogens to the MLN, we infected streptomycin pretreated $Flt3^{-/-}$ mice, that lack $CD103^+CD11b^+$ lamina propria DCs and have reduced numbers of $CD103^+CD11b^-$ PP DCs, with *Salmonella Typhimurium* either orally or systemically. Strikingly, two days after oral infection, *Salmonella* dissemination to the MLN (Fig. 6A) and spleen (not shown) was strongly reduced in $Flt3^{-/-}$ mice compared to wild type mice controls, while bacterial loads in the SB were comparable between each group. In contrast, the rate of *Salmonella* dissemination upon systemic infection was similar in mutant and wild type mice (not shown). Since in orally infected streptomycin-pretreated mice, *Salmonella* invades mainly though the lamina propria and not PP (Barthel et al., 2003), these results suggest that $CD103^+CD11b^+$ DCs are the main DC population that transports *Salmonella* from the intestinal tract to the MLN. Reduced bacterial dissemination to the MLN was also observed in $CCR7^{-/-}$ mice further supporting the key role of tissue migratory DCs in the transport and dissemination of intestinal pathogens to the draining LN (Fig. 6B). Altogether, these results establish the key role of $CD103^+CD11b^+$ lamina propria DCs in the transport of pathogens to the MLN.

Discussion

Our results establish the dual origin of the DC network that populates the intestinal mucosa in the steady state. Here we show that the lamina propria DC network consists of DCs derived from monocytes and pre-DCs. Lamina propria DC derived from pre-DCs are migratory, and participate in antigen trafficking and immuno-surveillance. The function of the monocyte-derived mucocsal DCs remains to be elucidated.

$CD103^+$ and $CX3CR1^+$ DCs represent two distinct mucosal DC subsets in the lamina propria. CX3CR1 is expressed mainly by lamina propria $CD103^-CD11b^+$ DCs, while CD103 is expressed on $CX3CR1^-CD11b^+$ lamina propria DCs and $CD11b^-CD8\alpha^+$ DCs in the PP. CX3CR1 is also expressed on $MHCII^{h}iCD11c^{lo}$ DCs, a population initially characterized as lamina propria macrophages (Denning et al., 2007), that accumulates mainly in the intestinal muscularis and the serosa distant from the lumen.

$CD103^+CD11b^+$ lamina propria DCs arise from CDP and pre-DCs independently of monocytes. CDP localizes in the BM and has been shown to give rise to pre-DC (Liu et al., 2009) and plasmacytoid DCs in the blood and to classical DCs in the spleen and peripheral LN but not to monocytes or macrophages (Naik et al., 2007; Onai et al., 2007c), while pre-DCs have lost a plasmacytoid DC potential and give rise only to lymphoid organ DCs (Liu et al., 2009) . Here we show that in addition to giving rise to lymphoid organ DCs, CDP and pre-DCs also give rise to $CD103^+CD11b^+$ but not $CD103^-CD11b^+$ lamina propria DCs.

Flt3 ligand is a key cytokine in DC differentiation *in vivo*. CDP and pre-DCs express high levels of Flt3 (Liu et al., 2009; Naik et al., 2007; Onai et al., 2007c) and the loss of Flt3 expression among hematopoietic progenitors coincides with the loss of DC differentiation potential (Onai et al., 2007a). Conversely, enforced Flt3 gene expression among Flt3 negative hematopoietic progenitors rescues their DC differentiation potential (Onai et al., 2006) establishing the instructive role of Flt3 in DC differentiation in the BM. In addition to its role on progenitors, Flt3 also controls the homeostasis of differentiated DCs in lymphoid organs (Waskow et al., 2008). Consistent with the key role of Flt3 in DC differentiation *in vivo*, our

results establish that $CD103^+CD11b^+$ lamina propria DCs represent the DC population most strongly affected in the absence of Flt3 or its ligand.

In addition to Flt3 ligand, our results reveal that GM-CSF controls the development of $CD103^+CD11b^+$ lamina propria DCs establishing for the first time the role of GM-CSF in DC development *in vivo* in the steady state. GM-CSF is a key cytokine to generate DCs *in vitro*, in mice and humans (Banchereau and Steinman, 1998). Therefore it came as a surprise that mice that lack GM-CSF or its receptor do not have any DC developmental defect in lymphoid organs (Vremec et al., 1997). Subsequent results suggested that GM-CSF participates in the development of DCs in inflamed lymphoid tissue (Naik et al.). Here we show that GM-CSF controls the differentiation of lamina propria DCs in the steady state.

In contrast to $CD103^+CD11b^+$ lamina propria DCs, $CD103^-CD11b^+$ DCs arise from $Ly6C^{hi}$ monocytes and not from CDP or pre-DCs. Upon adoptive transfer, $Ly6C^{hi}$ monocytes have been shown to shuttle back to the BM to give rise to blood circulating $Ly6C^{lo}$ monocytes (Varol et al., 2007). Therefore, it is possible that $Ly6C^{hi}$ monocyte contribution to lamina propria DCs is mediated mainly through $Ly6C^{lo}$ monocytes. Consistent with their high M-CSFR expression, differentiation of $CD103^-CD11b^+$ lamina propria DCs is strongly dependent on M-CSFR ligands. M-CSFR plays a key role in macrophage differentiation and is thought to control the differentiation, proliferation and survival of macrophages *in vivo* (Pixley and Stanley, 2004). One of the M-CSFR ligand, M-CSF, is expressed in the BM but also in the lamina propria (Klebl et al., 2001) suggesting a potential role for M-CSF not only at the progenitor level but also at the tissue site. More recently, a second M-CSFR ligand has been identified in mice and humans. This ligand named interleukin-34 binds to M-CSFR with higher affinity than M-CSF (Lin et al., 2008). The exact contribution of each M-CSFR ligand to lamina propria DC development *in vivo* remains to be established. It also remains to be established whether M-CSFR signaling is required mainly at the progenitor level in the BM or at the tissue site. These results extend the role of M-CSFR in hematopoietic cell development and establish that in addition to its role in the development of macrophages and epidermal Langerhans cells, M-CSFR also controls the development of a specific monocyte derived DC subset in the lamina propria.

In addition to giving rise to spleen and peripheral lymphoid organ DCs, CDP and pre-DCs also give rise to $CD103^+CD11b^-$ PP DCs. $CD103^+CD11b^-$ DCs are also strongly dependent on Flt3 ligand, but in contrast to lamina propria CD103+$CD11b^+$ DCs, they develop independently of GM-CSF. These results are consistent with the data showing that the absence of GM-CSF or GM-CSFR does not affect the development of DCs in quiescent lymphoid organs in mice (Vremec et al., 1997).

Altogether these results establish for the first time the concomitant contribution of monocytes and committed DC precursors to the non-lymphoid tissue DC pool in the steady state and pose the question of the functional relevance of this dual DC origin. The results presented here reveal that one striking functional difference between the two DC lineages resides in their ability to survey the gut. Our data show that pre-DC-derived $CD103^+CD11b^+$ lamina propria DCs constitutively express high CCR7 levels, while monocyte-derived $CD103^-$ $CD11b^+$ lamina propria DCs express no or low CCR7 levels in the steady state. Consistently, $CD103^+CD11b^+$ lamina propria DCs are the predominant DC population affected in the MLN of CCR7 deficient mice. These results are consistent with previous studies showing that $CD103^+$ DCs are the main DC population that present oral antigens to MLN T cells in the steady state (Jaensson et al., 2008). The potency of $CD103^+$ DCs to induce T regulatory cells was shown to be dependent on their superior ability to produce retinoic acids as compared to the $CD103^-$ DCs (Coombes et al., 2007; Sun et al., 2007). The unique ability of $CD103^+CD11b^+$ DCs to migrate to the draining LN in the steady state may provide another

advantage over $CD103^{-}CD11b^{+}$ lamina propria DCs to present luminal antigens in MLN in a tolerogeneic context.

In contrast to $CD103^{+}CD11b^{+}$ lamina propria DCs, monocyte-derived lamina propria DCs do not substantially migrate to the draining LN in the steady state. It is, however, surprising that these cells uniquely express high levels of CX3CR1, a molecule shown to control the formation of DC protrusions and the sampling of luminal antigens (Niess et al., 2005; Rescigno et al., 2001a), raising the question as to the purpose of antigen sampling if antigens are not to be transported to the LN. One possibility is that CX3CR1 dependent sampling is more physiologically relevant during intestinal inflammation as DC protrusions although present in the steady state dramatically increase during infection (Chieppa et al., 2006). Another possibility is that the capture of luminal antigens by monocyte-derived DCs triggers cytokine secretion that modulates tissue immune environment either locally or through the control of $CD103^{+}CD11b^{+}$ DC migration to the MLN. Another tempting hypothesis is that $CD103^{-}CD11b^{+}CX3CR1^{hi}$ DCs provide luminal antigens to $CD103^{+}CD11b^{-}$ DCs, a possibility that is currently being tested in the laboratory.

$CD103^{+}CD11b^{+}$ lamina propria DCs are located in close proximity to the epithelial layer suggesting that they too might be able to sample antigens. The integrin CD103 is a ligand for E-cadherin, an adhesion molecule expressed by epithelial cells (Cepek et al., 1994) may promote the homing of $CD103^{+}CD11b^{+}$ lamina propria DCs to the gut epithelia facilitating the ability of the $CD103^{+}CD11b^{+}$ lamina propria DCs to sample cell-associated antigens. Another possibility is that they acquire antigens directly through PP-independent M cells (Jang et al., 2004) or through cross-presentation of the $CD103^{-}CD11b^{+}CX3CR1^{+}$ lamina propria DCs as suggested above.

Using a *Salmonella* Typimurium oral infection model in streptomycin-pretreated mice to enforce pathogen invasion through the epithelia rather than PP (Barthel et al., 2003), we also established the superior ability of $CD103^{+}CD11b^{+}$ lamina propria DCs to transport gut pathogens to the MLN. Although this model was described to affect mostly the large bowel, we consistently observed distal SB inflammation starting one day after the infection (not shown). Expression of TLR5 by gut DCs was shown to play a key role in DC transport of *Salmonella* to the draining LN (Uematsu et al., 2006). Although, we found that both monocyte-derived and CDP-derived DCs express TLR5 (not shown), $CD103^{+}CD11b^{+}$ lamina propria DCs were the first to transport the pathogen to the MLN. DC ability to transport antigens from the intestinal tract to the MLN, although critical to initiate systemic immunity against gut pathogens, can be used by facultative pathogens to disseminate in the host. This was most clearly shown in a model of *Salmonella* Typhimurium infection, in which the inability of $TLR5^{-/-}$ DCs to transport the pathogen to the MLN improved the infection outcome by reducing the systemic dissemination of the pathogen (Uematsu et al., 2006). It is likely that the specific depletion of $CD103^{+}CD11b^{+}$ lamina propria DCs may also improve mice survival upon oral *Salmonella* infection by reducing or delaying pathogen transport in the MLN.

Altogether, these results identify for the first time the dual origin of the lamina propria DC network. Here we show that $CD103^{-}CD11b^{+}$ lamina propria DCs arise from circulating monocytes under the control of M-CSFR ligand and to a lesser degree Flt3 ligand, while $CD103^{+}CD11b^{+}$ lamina propria DCs derive from DC restricted progenitors under the control of Flt3 ligand and GM-CSF. In contrast to monocyte-derived DCs, lamina propria DCs that arise from pre-DCs constitutively migrates to the MLN in the steady state, and excel in the induction of peripheral Foxp3+ T regulatory cells (Coombes et al., 2007; Sun et al., 2007). They also represent the first DC population to migrate to the draining LN in the inflamed setting, likely playing a key role in gut immuno-surveillance. These results underline the developmental and functional diversity of the mucosal DC network and suggest that oral

immunization strategies could be substantially optimized by targeting specific DC populations in the lamina propria.

Materials and methods

Mice

C57BL/6 (CD45.2$^+$), congenic CD45.1$^+$ C57BL/6, transgenic M-CSFR-GFP C57BL/6 (Burnett et al., 2004) and OVA TCR transgenic OT II mice were purchased from the Jackson Laboratory (Jackson Laboratory, Bar Harbor, ME). CX3CR1$^{GFP/GFP}$ C57BL/6 knock in mice were provided by Dr. Dan Littman (Skirball Institute, New York, NY) and bred with WT C57BL/6 mice to obtain heterozygote CX3CR1$^{GFP/-}$ mice. Transgenic C57BL/6 mice expressing an enhanced yellow fluorescence protein (EYFP) reporter under the control of the CD11c promoter were generated as described (Lindquist et al., 2004). Flt3$^{-/-}$ C57BL/6 mice were kindly provided by Dr. Ihor Lemischka (Mount Sinai School of Medicine, New York, NY). Id2$^{-/-}$ were kindly provided by Dr. Yoshifumi Yokota (University of Fukui, Japan). M-CSFR$^{-/-}$ FVB/NJ mice and M-CSFR$^{+/-}$ C57BL/6 were kindly provided by Dr. Richard Stanley (Albert Einstein College of Medicine, Bronx, NY). Flt3L$^{-/-}$ mice were purchased from Taconic (Taconic Farms, Hudson, NY). All mice were analyzed between 8–12 weeks of age with the exception for MCSFR$^{-/-}$ mice which were analyzed at 3 weeks of age due to their early lethality. Mice were housed in a specific pathogen-free environment at Mount Sinai School of Medicine and were used in accordance with protocols approved by the Institutional Animal Care and Utilization committee.

Isolation of intestinal cell suspensions

To prepare single intestinal cell suspension, part of small bowel (SB) including jejunum and ileum, or large bowel (cecum and colon) were excised by separation from the mesentery. Intestines were opened with scissors along the intestinal length. Next, intestinal tissues were incubated on a shaker in complete medium (CM, 2% FBS in Ca^{2+}, Mg^{2+} free HBSS, Cellgro, Herndon, VA) in the presence of 1 mM DTT (Sigma-Aldrich, St. Louis, MO) at 37° C for 20 min followed by incubation with 1.3 mM EDTA (Cellgro) in CM at 37°C for 1 h. The supernatants containing intestinal epithelial cell (IEC) with some superficial villi cells, referred to as the “IEC fraction”, were collected and analyzed by flow cytometry. To analyze DC subset distribution in different anatomical compartments of SB, PP were excised with scissors; the intestinal muscularis covered by the serosa was peeled from the sub-mucosa with the use of fine surgical forceps and a dissection microscope (model SZ51; Olympus). SB villi representing intestinal LP were scraped from the underlying submucosa. Isolated tissues were collected, digested with 0.2 mg/ml of type IV collagenase (Sigma-Aldrich) at 37°C for 1 h. Tissues were then homogenized, filtered and washed. To enrich CD11c^{hi} LP DCs, the PP were always excised and the intestinal muscularis was routinely separated from the rest of the tissue (mucosa and submucosa) and either discarded or subjected to a separate analysis. Single cells suspensions were stained with mAbs and analyzed by flow cytometry. MLN and splenic cell suspensions were prepared by digestion with type IV collagenase for 20 min.

Mixed bone marrow chimeras

Eight-week old CD45.1$^+$ C57BL/6 recipient mice were lethally irradiated with 1,200 rad delivered in two doses of 600 rad each (Cesium source) 3 h apart and injected i.v. with 5 × 10^5 bone marrow (BM) cells or fetal liver cells. Mice were reconstituted with a mixture of 50% WT CD45.1$^+$ and 50% FLT3$^{-/-}$, GMCSFR-$^{-/-}$ or WT CD45.2$^+$ BM cells or with 10% WT CD45.1$^+$ BM cells and 90% CD45.2$^+$ fetal liver cells isolated from M-CSFR$^{-/-}$ or control littermates. E14.5 fetal liver was used in this case because C57BL/6 M-CSFR$^{-/-}$ mice are embryonically lethal. CD45.1$^+$ C57BL/6 recipients transplanted with 100% WT CD45.2$^+$ BM were used to control complete replacement of recipient hematopoietic cells with donor BM

derived cells. In all transplanted mice, engraftment was assessed by measuring the relative numbers of donor cells among blood $SSC^{lo}CD115^{+}Ly6C/G^{hi}$ monocytes or $SSC^{int}CD11b^{+}Ly6C/G^{+}$ granulocytes 3 to 4 weeks after transplantation.

Parabiosis

Parabiotic mice were generated as described previously (Wright et al., 2001). Each pair of parabiotic mice consisted of $CD45.1^{+}$ and $CD45.2^{+}$ WT C57BL/6 parabionts with shared blood circulation. Two weeks after initiation of parabiosis, mice were sacrificed and subjected to tissue analysis. To confirm efficient blood mixing in parabiotic mice, the % of $CD45.1^{+}$ and $CD45.2^{+}$ among blood $CD45^{+}$ leukocytes was analyzed in each animal.

Salmonella infection in vivo

The naturally streptomycin resistant wild type *Salmonella enterica* subspecies 1 serovar Typhimurium (*S.* Typhimurium) SL1344 strain (Hoiseth and Stocker, 1981) was grown in Luria-Bertani (LB) broth for 18 hrs, harvested by centrifugation and resuspended in cold PBS. Bacterial concentration was estimated by measuring optical density at 420 nm and confirmed by plating bacterial dilutions of LB agar plates. OD_{420} of 1 is equal to 1×10^{8} CFU/ml (Singh et al., 2000). To induce salmonella-dependent enterocolitis mice were infected according to the previously described protocol (Barthel et al., 2003). Briefly, mice were pretreated by gavage with 20 mg of streptomycin. Twenty four h later, mice were orally infected with 5×10^{7} CFU of streptomycin resistant wild type *S.* Typhimurium. To assess the mortality rate from systemic infection, mice were injected with 5×10^{4} *S.* Typhimurium intraperitoneally (i/p). To detect intracellular *S.* Typhimurium in MLN DCs, mice were infected i/p with 1×10^{6} CFU of *S.* Typhimurium and sacrificed 18 h post-infection. Live bacterial loads in the intestinal tissues and MLN were determined by plating serial dilutions of homogenized tissues on LB agar plates supplemented with 50 μg/ml of streptomycin (Calbiochem, Gibbstown, NJ).

Flow cytometry

Multi-parameter (up to 7 colors) analyses of stained cell suspensions were performed on the LSR II (Becton Dickinson, San Jose, CA) and analyzed with FlowJo software (Tree Star, Ashland, OR). Fluorochrome or biotin-conjugated monoclonal antibodies (mAbs) specific to mouse B220 (clone RA3-6B2), CD8α (clone 53-6.7), MHC Class II (I-A/I-E, clone M5/114.15.2), CD103 (clone 2E7), CD11b (clone M1/70), CD11c (clone N418), CD45 (clone 30F11), CD45.1 (clone A20), CD45.2 (clone 104), M-CSFR (also called CD115) (clone AFS98), Ly6C/G (clone RB6-8C5), Vα2 (clone B20.1), the corresponding isotype controls and the secondary reagent PE-Cy7–conjugated streptavidin were purchased either from BD Biosciences or eBioscience (San Diego, CA). Anti-F4/80 (A3-1) mAb was purchased from Serotec (Raleigh, NC). To detect intracellular *S.* Typhimurium viable cells were stained for the surface markers, fixed and permeabilized using the BD Cytofix/Cytoperm kit (BD Biosciences) according to the manufacturer's protocol and incubated with the FITC labeled anti-*Salmonella* common structural antigens CSA-1 polyclonal Ab (Kirkegaard & Perry Laboratories, Gaithersburg, MD) or an isotype control Ab.

Cell sorting

Single cell suspensions of viable cells were stained for the surface markers and individual DC subsets were sorted with FACS-Vantage Flow Cytometer/Cell Sorter (Becton Dickinson) according to determined phenotypes to achieve 98% purity. Cooling system was applied to prevent excessive cell activation and death. One, two or three way sort was performed. Purified cell phenotypes were as followed: $MHCII^{hi}CD11c^{hi}CD11b^{-}CD103^{+}$, $MHCII^{hi}CD11c^{hi}CD11b^{+}CD103^{+}$ and $MHCII^{hi}CD11c^{hi}CD11b^{+}CD103^{-}$ SB LP DCs, $MHCII^{hi}CD11c^{+}CD11b^{+}CD103^{+}$, $MHCII^{hi}CD11c^{+}CD11b^{+}CD103^{-}$,

MHCII^{hi}CD11c^{+}CD11b^{-}CD103^{+} MLN DCs, MHCII^{hi}CD11c^{+}CD11b^{+} splenic DCs or MHCII^{+}CD11c^{-}CD11b^{-}B220^{+} splenic B cells. To sort cells from infected tissues, cell suspension were fixed prior to sorting as described above.

Cytospin of sorted cells

To examine DC morphology viable sorted cells were spun onto glass slides, dried overnight and stained with Giemsa. Images were analyzed using the Nikon Eclipse E800 microscope (Nikon, Japan) at 600x magnification. To view infected cells, MLN cell suspensions were stained for DC cell surface markers, fixed and sorted. Purified DC subsets were stained with the FITC labeled anti-*Salmonella* CSA-1 polyclonal Ab (Kirkegaard & Perry Laboratories), spun onto glass slides and mounted with the Vectashield Mount Medium containing DAPI (Vector Laboratories, Burlingame, CA). Images were acquired at 600x magnifications using a Leica DMRA2 fluorescence microscope with a Hamamatsu CCD digital camera and analyzed using Openlab software (Improvision, Waltham, MA).

Immunofluorescent analysis of intestinal cross-sections

Prior to organ collection, *CD11c-EYFP* transgenic mice or *CX3CR1*$^{GFP/-}$ knock-in mice were perfused intravenously with 2% formaldehyde / 20% sucrose in PBS solution to preserve intracellular GFP/YFP. Organs were then harvested and rinsed in PBS before freezing in optimum cutting temperature compound. Six μm thick cross-sections of terminal ileum were placed on Superfrost/Plus microscope slides (Fisher Scientific, Pittsburgh, PA) and incubated with 5% goat serum, 0.5% Triton in PBS for 30 min followed by an overnight staining with the primary antibody directed against CD103 (eBioscience). Slides were then washed in PBS with 0.1% Triton (Sigma-Aldrich) and stained for 60 min with the secondary goat anti-Armenian hamster IgG-Biotin followed by Streptavidin-Cy3 (*CX3CR1*$^{GFP/-}$ mice) or Streptavidin-Cy5 (*CD11c-EYFP* mice) from Jackson Immunoresearch Laboratories, West Grove, PA. Slides were mounted in Vectashield Mount Medium containing DAPI (Vector Laboratories). Images were acquired at 200x and 400x magnification using a Leica DMRA2 fluorescence microscope with a Hamamatsu CCD digital camera and analyzed with Openlab software (Improvision).

T cell proliferation assay in vitro

Live 103^{+}CD11b^{+} and CD103^{-}CD11b^{+} SB LP DCs, splenic DCs or splenic B cells were sorted as described above. 1×10^{4} DCs were supplemented with 1 μg/ml of $OVA_{323–339}$ peptide and co-cultured with 5×10^{4} CD11c^{-}CD4^{+} OT-II T cells labeled with 5 μM CFSE (Molecular Probes/Invitrogen, Carlsbad, CA) in CM (RPMI, Cellgro; 10% FBS, 0.1% b-2ME, Sigma-Aldrich; 1% penicillin, 0.1% fungizone, Gibco/Invitrogen). Four days later the proliferation of OT-II T cells (CD11c^{-}Vα2^{+}TCR^{+}) was assessed by measuring the dilution of the CFSE by flow cytometry.

MDP, CDP, pre-DC and monocyte transfer experiments

MDPs were sorted as lineage (CD3, TCRβ, CD19, B220, Gr1, CD11b, CD11c, NK1.1, Ter119, pDCA, MHCII) negative, CD115^{+}Flt3^{+}c-kit^{hi} cells from the BM of CD45.1^{+} C57BL/6 mice. CDPs were sorted as lineage^{-}CD115^{+}Flt3^{+}c-kit^{lo} cells from the BM of CD45.1^{+} C57BL/6 mice, as described in (Onai et al., 2007c). Pre-DCs were sorted as CD3^{-}CD19^{-}NK1.1^{-}Ter119^{-}B220^{-}IA^{-} CD11c^{int}Flt3^{+}SIRPα^{int} from the BM of CD45.1^{+} C57BL/6 mice, as described in (Liu et al., 2009). Ly6C^{hi} monocytes were sorted as described in (Ginhoux et al., 2006) from CD45.1^{+} bone marrow. 3×10^{5} MDP, 5×10^{5} CDP and between 1.5 and 2×10^{6} monocytes were injected i.v. into either untreated or diphtheria toxin (DT) treated CD45.2^{+} CD11c-DTR C57BL/6 transgenic mice. DT (List Biological Laboratories, Campbell, CA) was reconstituted and stored according to the manufacturer's protocol. To deplete

CD11c^{hi} cells CD11c-DTR mice were injected with 5 ng/g of DT intraperitoneally 12 h prior to cell transfer.

Quantitative PCR

Total RNA from sorted DC subsets was extracted using the RNeasy micro Kit (Qiagen, Valencia, CA) according to the manufacturer's instructions. Reverse transcription was performed using RNA from 5×10^4 to 1×10^5 cells and RNA concentration was standardized for all the samples. Quantitative PCR was conducted in duplicates. Relative expression levels were calculated as 2^(Ct Ubiquitin - Ct gene) using Ubiquitin RNA as the endogenous control. To confirm the results, two distinct sets of primers for mouse CCR7 were used in qPCR analysis. The sequences for the CCR7 primers were: CCR7 F1: 5′-CACGCTGAGATGCTCACTGG-3', CCR7 R1: 5'-CCATCTGGGCCACTTGGA-3'; CCR7 F2: 5'-TCCAGGCACGCAACTTTGA-3', CCR7 R2: 5'-CCACCACGGCAATGATCAC-3'. PCR primers were ordered from Integrated DNA Technogies, USA.

Statistical analysis

Data are presented as mean ± SD. The statistical significance of differences between group means was determined with the Student's *t* test. *p*-values of <0.05 were considered significant.

Supplementary Material

Refer to Web version on PubMed Central for supplementary material.

Abbreviations used in this paper

DCs, dendritic cells; GM-CSFR, granulocyte macrophage colony stimulating factor receptor; Flt3, fms like thyrosine kinase 3; lamina propria, lamina propria; LN, lymph nodes; M-CSFR, macrophage colony stimulating factor receptor; MLN, Mesenteric lymph nodes.

References

Banchereau J, Steinman RM. Dendritic cells and the control of immunity. Nature 1998;392:245–252. [PubMed: 9521319]

Barthel M, Hapfelmeier S, Quintanilla-Martinez L, Kremer M, Rohde M, Hogardt M, Pfeffer K, Russmann H, Hardt WD. Pretreatment of mice with streptomycin provides a Salmonella enterica serovar Typhimurium colitis model that allows analysis of both pathogen and host. Infect Immun 2003;71:2839–2858. [PubMed: 12704158]

Burnett SH, Kershen EJ, Zhang J, Zeng L, Straley SC, Kaplan AM, Cohen DA. Conditional macrophage ablation in transgenic mice expressing a Fas-based suicide gene. J Leukoc Biol 2004;75:612–623. [PubMed: 14726498]

Cepek KL, Shaw SK, Parker CM, Russell GJ, Morrow JS, Rimm DL, Brenner MB. Adhesion between epithelial cells and T lymphocytes mediated by E-cadherin and the alpha E beta 7 integrin. Nature 1994;372:190–193. [PubMed: 7969453]

Chieppa M, Rescigno M, Huang AY, Germain RN. Dynamic imaging of dendritic cell extension into the small bowel lumen in response to epithelial cell TLR engagement. J Exp Med 2006;203:2841–2852. [PubMed: 17145958]

Coombes JL, Powrie F. Dendritic cells in intestinal immune regulation. Nat Rev Immunol 2008;8:435–446. [PubMed: 18500229]

Coombes JL, Siddiqui KR, Arancibia-Carcamo CV, Hall J, Sun CM, Belkaid Y, Powrie F. A functionally specialized population of mucosal CD103+ DCs induces Foxp3+ regulatory T cells via a TGF-beta and retinoic acid-dependent mechanism. J Exp Med 2007;204:1757–1764. [PubMed: 17620361]

Denning TL, Wang YC, Patel SR, Williams IR, Pulendran B. Lamina propria macrophages and dendritic cells differentially induce regulatory and interleukin 17-producing T cell responses. Nat Immunol 2007;8:1086–1094. [PubMed: 17873879]

Flores-Langarica A, Meza-Perez S, Calderon-Amador J, Estrada-Garcia T, Macpherson G, Lebecque S, Saeland S, Steinman RM, Flores-Romo L. Network of dendritic cells within the muscular layer of the mouse intestine. Proc Natl Acad Sci U S A 2005;102:19039–19044. [PubMed: 16361439]

Fogg DK, Sibon C, Miled C, Jung S, Aucouturier P, Littman DR, Cumano A, Geissmann F. A clonogenic bone marrow progenitor specific for macrophages and dendritic cells. Science 2006;311:83–87. [PubMed: 16322423]

Forster R, Schubel A, Breitfeld D, Kremmer E, Renner-Muller I, Wolf E, Lipp M. CCR7 coordinates the primary immune response by establishing functional microenvironments in secondary lymphoid organs. Cell 1999;99:23–33. [PubMed: 10520991]

Ginhoux F, Tacke F, Angeli V, Bogunovic M, Loubeau M, Dai XM, Stanley ER, Randolph GJ, Merad M. Langerhans cells arise from monocytes in vivo. Nat Immunol 2006;7:265–273. [PubMed: 16444257]

Hoiseth SK, Stocker BA. Aromatic-dependent Salmonella typhimurium are non-virulent and effective as live vaccines. Nature 1981;291:238–239. [PubMed: 7015147]

Huang FP, Platt N, Wykes M, Major JR, Powell TJ, Jenkins CD, MacPherson GG. A discrete subpopulation of dendritic cells transports apoptotic intestinal epithelial cells to T cell areas of mesenteric lymph nodes. J Exp Med 2000;191:435–444. [PubMed: 10662789]

Jaensson E, Uronen-Hansson H, Pabst O, Eksteen B, Tian J, Coombes JL, Berg PL, Davidsson T, Powrie F, Johansson-Lindbom B, Agace WW. Small intestinal CD103+ dendritic cells display unique functional properties that are conserved between mice and humans. J Exp Med 2008;205:2139–2149. [PubMed: 18710932]

Jakubzick C, Bogunovic M, Bonito AJ, Kuan EL, Merad M, Randolph GJ. Lymph-migrating, tissue-derived dendritic cells are minor constituents within steady-state lymph nodes. J Exp Med 2008;205:2839–2850. [PubMed: 18981237]

Jang MH, Kweon MN, Iwatani K, Yamamoto M, Terahara K, Sasakawa C, Suzuki T, Nochi T, Yokota Y, Rennert PD, et al. Intestinal villous M cells: an antigen entry site in the mucosal epithelium. Proc Natl Acad Sci U S A 2004;101:6110–6115. [PubMed: 15071180]

Johansson C, Kelsall BL. Phenotype and function of intestinal dendritic cells. Semin Immunol 2005;17:284–294. [PubMed: 15978836]

Johansson-Lindbom B, Svensson M, Pabst O, Palmqvist C, Marquez G, Forster R, Agace WW. Functional specialization of gut CD103+ dendritic cells in the regulation of tissue-selective T cell homing. J Exp Med 2005;202:1063–1073. [PubMed: 16216890]

Jung S, Aliberti J, Graemmel P, Sunshine MJ, Kreutzberg GW, Sher A, Littman DR. Analysis of fractalkine receptor CX(3)CR1 function by targeted deletion and green fluorescent protein reporter gene insertion. Mol Cell Biol 2000;20:4106–4114. [PubMed: 10805752]

Jung S, Unutmaz D, Wong P, Sano G, De los Santos K, Sparwasser T, Wu S, Vuthoori S, Ko K, Zavala F, et al. In vivo depletion of CD11c(+) dendritic cells abrogates priming of CD8(+) T cells by exogenous cell-associated antigens. Immunity 2002;17:211–220. [PubMed: 12196292]

Klebl FH, Olsen JE, Jain S, Doe WF. Expression of macrophage-colony stimulating factor in normal and inflammatory bowel disease intestine. J Pathol 2001;195:609–615. [PubMed: 11745698]

Lin H, Lee E, Hestir K, Leo C, Huang M, Bosch E, Halenbeck R, Wu G, Zhou A, Behrens D, et al. Discovery of a cytokine and its receptor by functional screening of the extracellular proteome. Science 2008;320:807–811. [PubMed: 18467591]

Lindquist RL, Shakhar G, Dudziak D, Wardemann H, Eisenreich T, Dustin ML, Nussenzweig MC. Visualizing dendritic cell networks in vivo. Nat Immunol 2004;5:1243–1250. [PubMed: 15543150]

Liu K, Victora GD, Schwickert TA, Guermonprez P, Meredith MM, Yao K, Chu FF, Randolph GJ, Rudensky AY, Nussenzweig M. In Vivo Analysis of Dendritic Cell Development and Homeostasis. Science. 2009

Macpherson AJ, Uhr T. Induction of protective IgA by intestinal dendritic cells carrying commensal bacteria. Science 2004;303:1662–1665. [PubMed: 15016999]

Merad M, Manz MG. Dendritic cell homeostasis. Blood 2009;113:3418–3427. [PubMed: 19176316]

Naik SH, Metcalf D, van Nieuwenhuijze A, Wicks I, Wu L, O'Keeffe M, Shortman K. Intrasplenic steady-state dendritic cell precursors that are distinct from monocytes. Nat Immunol. 2006

Naik SH, Sathe P, Park HY, Metcalf D, Proietto AI, Dakic A, Carotta S, O'Keeffe M, Bahlo M, Papenfuss A, et al. Development of plasmacytoid and conventional dendritic cell subtypes from single precursor cells derived in vitro and in vivo. Nat Immunol 2007;8:1217–1226. [PubMed: 17922015]

Niess JH, Brand S, Gu X, Landsman L, Jung S, McCormick BA, Vyas JM, Boes M, Ploegh HL, Fox JG, et al. CX3CR1-mediated dendritic cell access to the intestinal lumen and bacterial clearance. Science 2005;307:254–258. [PubMed: 15653504]

Ohl L, Mohaupt M, Czeloth N, Hintzen G, Kiafard Z, Zwirner J, Blankenstein T, Henning G, Forster R. CCR7 governs skin dendritic cell migration under inflammatory and steady-state conditions. Immunity 2004;21:279–288. [PubMed: 15308107]

Onai N, Obata-Onai A, Schmid MA, Manz MG. Flt3 in regulation of type I interferon-producing cell and dendritic cell development. Ann N Y Acad Sci 2007a;1106:253–261. [PubMed: 17360795]

Onai N, Obata-Onai A, Schmid MA, Manz MG. Flt3 in regulation of type-I interferon producing and dendritic cell development. Ann N Y Acad Sci. 2007b

Onai N, Obata-Onai A, Schmid MA, Ohteki T, Jarrossay D, Manz MG. Identification of clonogenic common Flt3+M-CSFR+ plasmacytoid and conventional dendritic cell progenitors in mouse bone marrow. Nat Immunol 2007c;8:1207–1216. [PubMed: 17922016]

Onai N, Obata-Onai A, Tussiwand R, Lanzavecchia A, Manz MG. Activation of the Flt3 signal transduction cascade rescues and enhances type I interferon-producing and dendritic cell development. J Exp Med 2006;203:227–238. [PubMed: 16418395]

Pixley FJ, Stanley ER. CSF-1 regulation of the wandering macrophage: complexity in action. Trends Cell Biol 2004;14:628–638. [PubMed: 15519852]

Rescigno M, Rotta G, Valzasina B, Ricciardi-Castagnoli P. Dendritic cells shuttle microbes across gut epithelial monolayers. Immunobiology 2001a;204:572–581. [PubMed: 11846220]

Rescigno M, Urbano M, Valzasina B, Francolini M, Rotta G, Bonasio R, Granucci F, Kraehenbuhl JP, Ricciardi-Castagnoli P. Dendritic cells express tight junction proteins and penetrate gut epithelial monolayers to sample bacteria. Nat Immunol 2001b;2:361–367. [PubMed: 11276208]

Singh SP, Williams YU, Klebba PE, Macchia P, Miller S. Immune recognition of porin and lipopolysaccharide epitopes of Salmonella typhimurium in mice. Microb Pathog 2000;28:157–167. [PubMed: 10702357]

Sun CM, Hall JA, Blank RB, Bouladoux N, Oukka M, Mora JR, Belkaid Y. Small intestine lamina propria dendritic cells promote de novo generation of Foxp3 T reg cells via retinoic acid. J Exp Med 2007;204:1775–1785. [PubMed: 17620362]

Sung SS, Fu SM, Rose CE Jr. Gaskin F, Ju ST, Beaty SR. A major lung CD103 (alphaE)-beta7 integrin-positive epithelial dendritic cell population expressing Langerin and tight junction proteins. J Immunol 2006;176:2161–2172. [PubMed: 16455972]

Uematsu S, Jang MH, Chevrier N, Guo Z, Kumagai Y, Yamamoto M, Kato H, Sougawa N, Matsui H, Kuwata H, et al. Detection of pathogenic intestinal bacteria by Toll-like receptor 5 on intestinal CD11c+ lamina propria cells. Nat Immunol 2006;7:868–874. [PubMed: 16829963]

Varol C, Landsman L, Fogg DK, Greenshtein L, Gildor B, Margalit R, Kalchenko V, Geissmann F, Jung S. Monocytes give rise to mucosal, but not splenic, conventional dendritic cells. J Exp Med 2007;204:171–180. [PubMed: 17190836]

Vremec D, Lieschke GJ, Dunn AR, Robb L, Metcalf D, Shortman K. The influence of granulocyte/macrophage colony-stimulating factor on dendritic cell levels in mouse lymphoid organs. Eur J Immunol 1997;27:40–44. [PubMed: 9021996]

Waskow C, Liu K, Darrasse-Jeze G, Guermonprez P, Ginhoux F, Merad M, Shengelia T, Yao K, Nussenzweig M. The receptor tyrosine kinase Flt3 is required for dendritic cell development in peripheral lymphoid tissues. Nat Immunol 2008;9:676–683. [PubMed: 18469816]

Worbs T, Bode U, Yan S, Hoffmann MW, Hintzen G, Bernhardt G, Forster R, Pabst O. Oral tolerance originates in the intestinal immune system and relies on antigen carriage by dendritic cells. J Exp Med 2006;203:519–527. [PubMed: 16533884]

Wright DE, Wagers AJ, Gulati AP, Johnson FL, Weissman IL. Physiological migration of hematopoietic stem and progenitor cells. Science 2001;294:1933–1936. [PubMed: 11729320]

Yrlid U, Jenkins CD, MacPherson GG. Relationships between distinct blood monocyte subsets and migrating intestinal lymph dendritic cells in vivo under steady-state conditions. J Immunol 2006;176:4155–4162. [PubMed: 16547252]

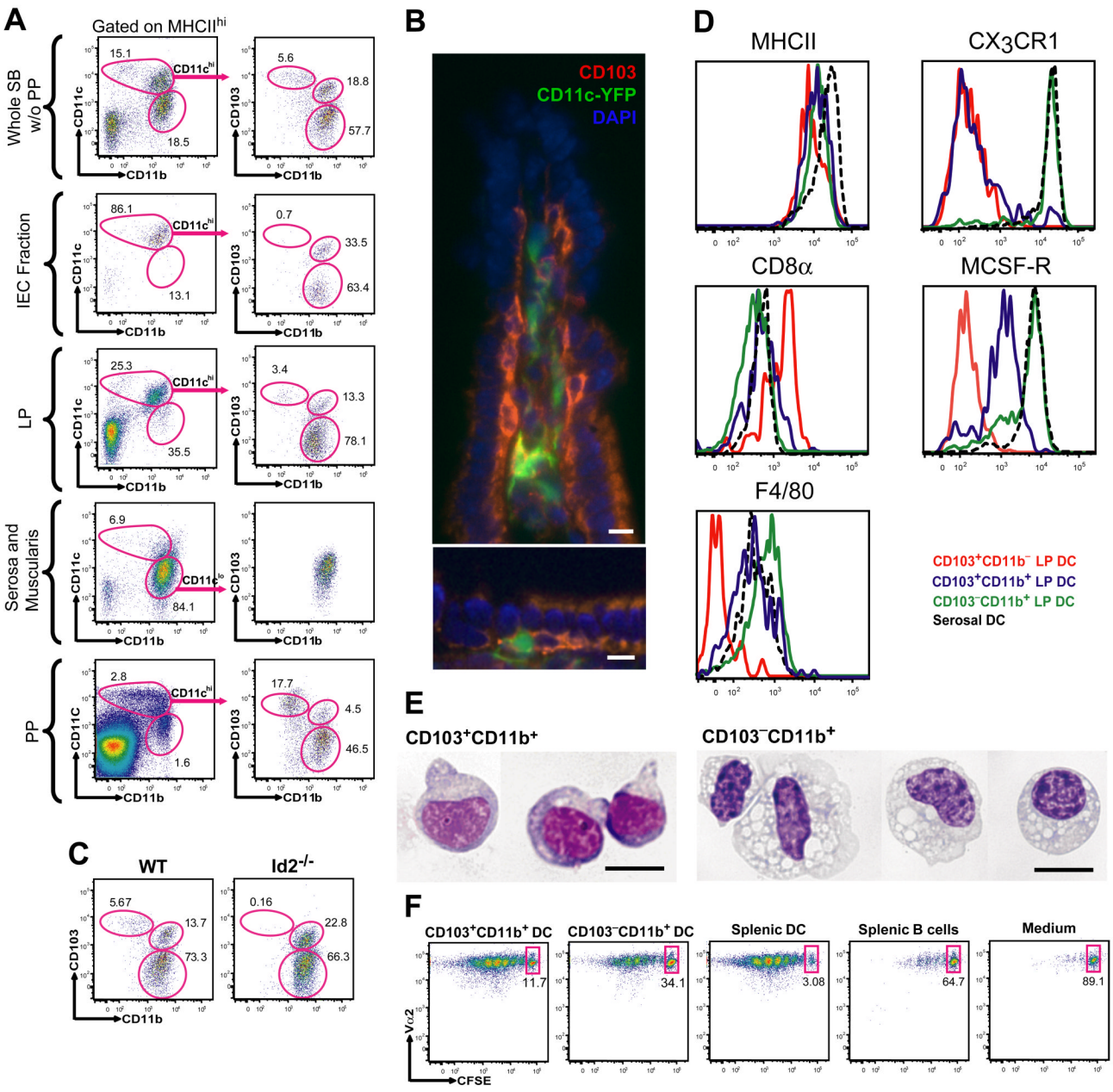

Figure 1. Characterization of phenotypically distinct DC subsets in the small bowel

A. Single cell suspensions prepared from different anatomical compartments of the small bowel (SB) including the IEC fraction, lamina propria (LP), serosa with the intestinal muscularis and PP were analyzed by seven color flow cytometry. The results were compared to the whole SB depleted of PP (SB without (w/o) PP). To define $CD11c^{hi}$ and $CD11c^{lo}$ DCs, gates were set on viable $DAPI^{-}CD45^{+}MHCII^{hi}$ cells. $CD11c^{hi}$ DCs were further divided into $CD103^{+}CD11b^{-}$, $CD103^{+}CD11b^{+}$ and $CD103^{-}CD11b^{+}$ DCs as indicated in the dot plots. Dot plots in the left column show the % of $CD11c^{hi}$ and $CD11c^{lo}$ DCs among total $DAPI^{-}CD45^{+}MHCII^{hi}$ cells. Dot plots in the right column show the % of $CD103^{+}CD11b^{-}$, $CD103^{+}CD11b^{+}$ and $CD103^{-}CD11b^{+}$ DCs among total $MHCII^{hi}CD11c^{hi}$ or $MHCII^{hi}CD11c^{lo}$ (serosa and muscularis) DCs. **B**. Images show the distribution of

$CD103^+CD11c\text{-}YFP^+$ cells in the villi of distal SB from *CD11c-EYFP* transgenic mice. Magnification 400x. Scale bar 10 nm. **C**. Dot plots show the % of $CD103^+CD11b^-$, $CD103^+CD11b^+$ and $CD103^-\text{-}CD11b^+$ DCs among $CD45^+MHCII^{hi}CD11c^{hi}$ cells in the SB depleted of PP in WT mice and in the total SB of $Id2^{-/-}$ mice. **D.** Overlay histograms show the differential MHCII, CD8α, CX3CR1, M-CSFR and F4/80 expression among each intestinal DC subset. **E**. Images show purified $CD103^+CD11b^+$ and $CD103^-CD11b^+$ SB LP DCs spun onto glass slides and stained with Giemsa. Magnification 600x. Scale bar 10 nm. **F**. CFSE labeled OTII cells were cultured with purified $CD103^+CD11b^+$ or $CD103^-CD11b^+$ SB LP DCs, splenic DCs or splenic B cells pulsed with OVA-peptide. Numbers are the % of OTII cells that have not proliferated in each group (representative data of two independent experiments done in triplicates).

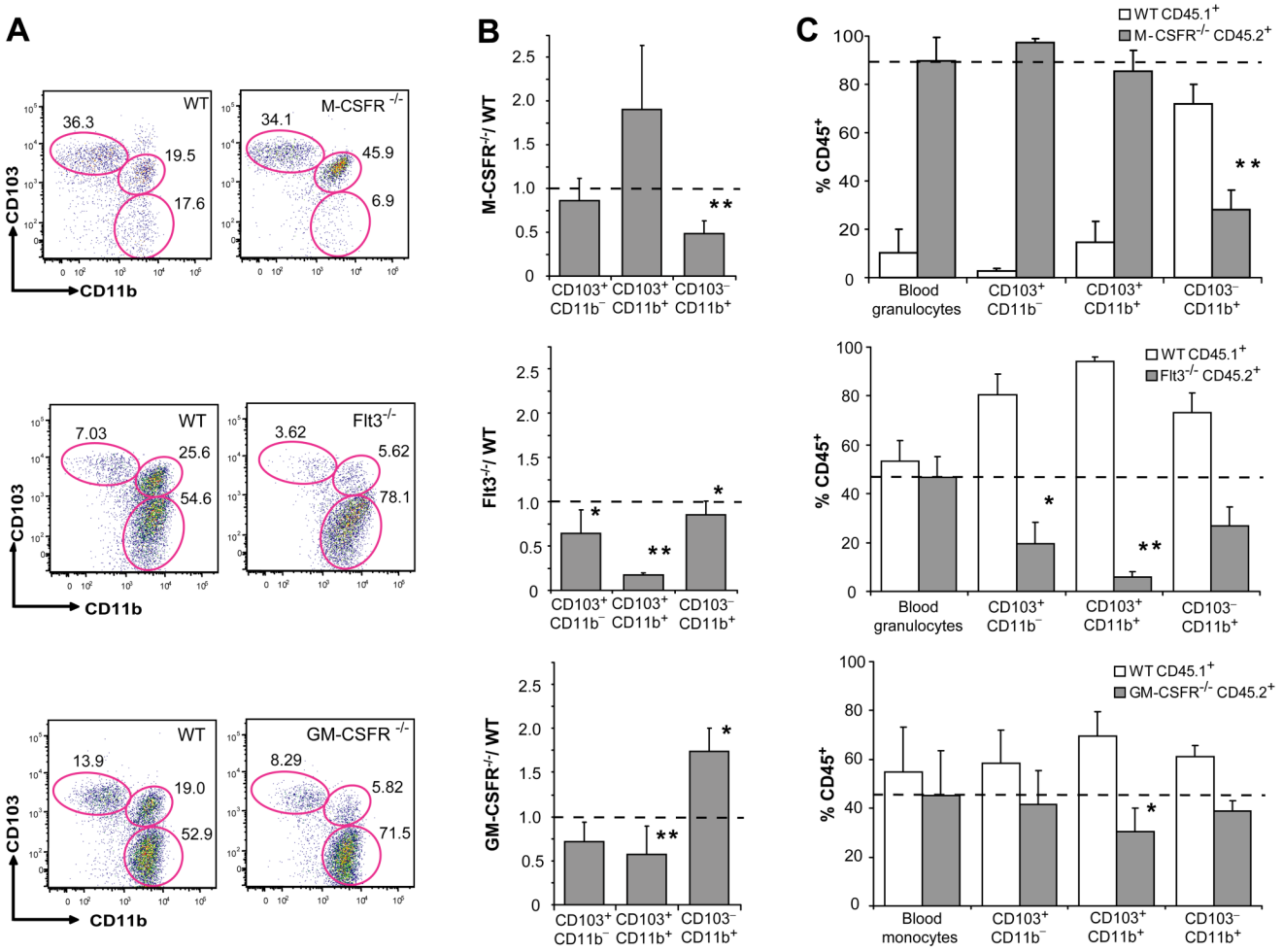

Figure 2. M-CSFR, Flt3 and GM-CSFR control the development of LP DCs

A. Dot plots show the % of $CD103^+CD11b^-$, $CD103^+CD11b^+$ and $CD103^-CD11b^+$ cells among $DAPI^-CD45^+MHCII^{hi}CD11c^{hi}$ SB LP DCs in M-$CSFR^{-/-}$, $Flt3^{-/-}$ and GM-$CSFR^{-/-}$ mice (right panels) or control WT littermates (left panels). PP were excised from the SB of $Flt3^{-/-}$, GM-$CSFR^{-/-}$ and control littermates, but not from the SB of M-$CSFR^{-/-}$ and their $MCSFR^{+/+}$ control littermates. **B**. Bar graphs show the relative change of absolute cell counts among SB LP DC subsets in M-$CSFR^{-/-}$, $Flt3^{-/-}$ and GM-$CSFR^{-/-}$ mice compared to WT mice. Error bars represent mean +/− SD from 4 (M-$CSFR^{-/-}$) to 6 ($Flt3^{-/-}$ and GM-$CSFR^{-/-}$) combined experiments. (*) − $0.05>p>0.005$, (**) − $p<0.005$. **C**. WT $CD45.1^+$ mice were lethally irradiated and reconstituted with a mixture of 1:1 $CD45.1^+$ WT and $CD45.2^+$ $Flt3^{-/-}$ or GM-$CSFR^{-/-}$ BM cells or with a mixture of 1:10 $CD45.1^+$ WT and $CD45.2^+$ $MCSFR^{-/-}$ fetal liver cells. Bar graphs show the % of $CD45.2^+$ KO and $CD45.1^+$ WT cells among blood cells (granulocytes or monocytes) used as a control and each SB LP DC subset. Error bars represent means +/− SD from 3 simultaneously analyzed experiments. (*) − $0.05>p>0.005$, (**) − $p<0.005$ as compared to the chimerism of blood granulocytes or monocytes.

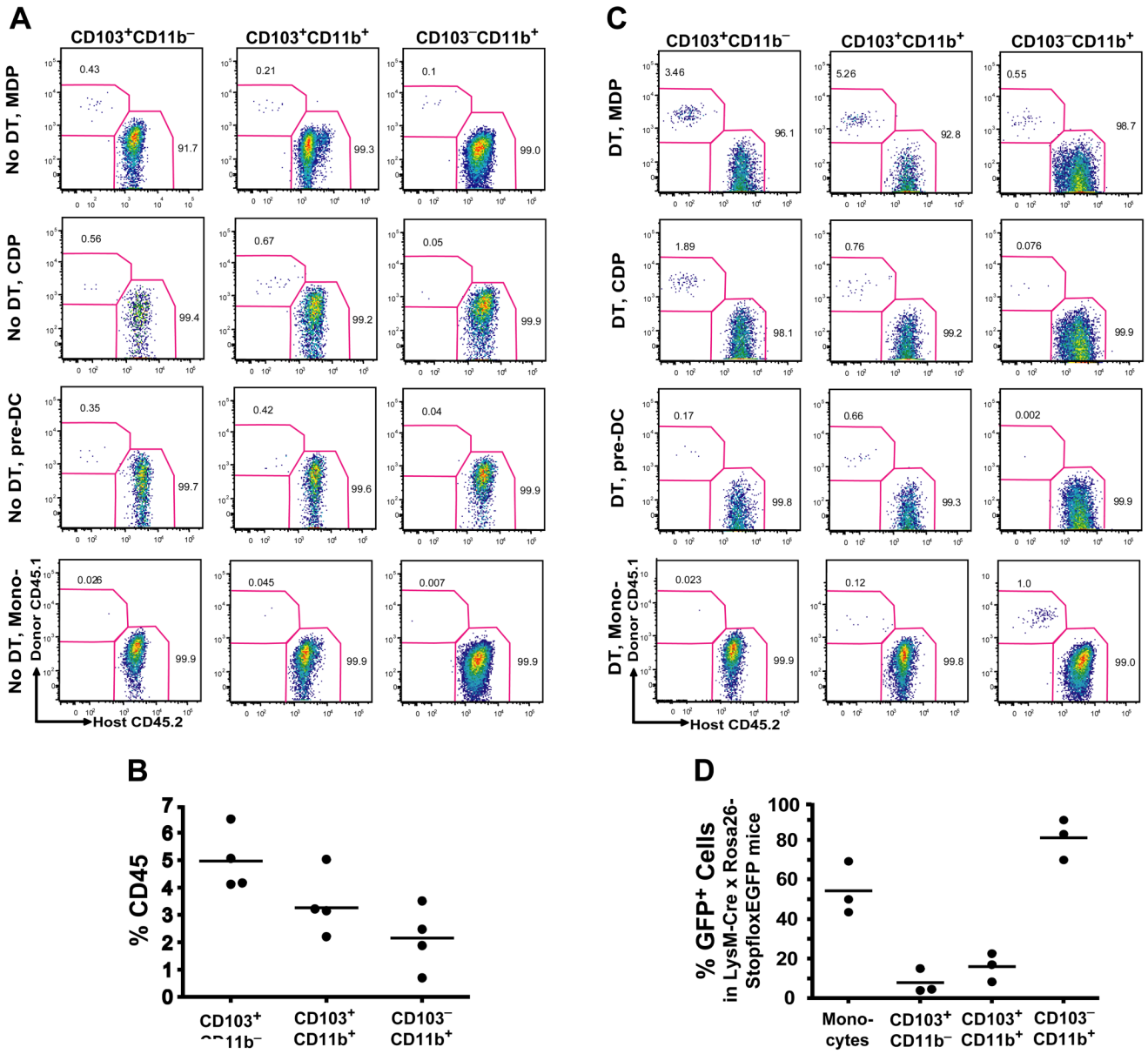

Figure 3. Origin of LP DCs

A. Untreated (No DT) CD45.2$^+$ CD11c-DTR recipients were injected i.v. with MDP, CDP, pre-DC or Ly6C^{hi} monocytes (mono-) purified from the BM of CD45.1$^+$ WT mice. Dot plots show the % of donor-derived CD45.1$^+$ cells among each SB LP DC subset seven days after adoptive transfer and represent three to four independent experiments (n=1 to 2). **B. Turnover of LP DCs in parabiotic mice**. Each parabiotic pair consisted of a CD45.1$^+$ and CD45.2$^+$ WT mouse with shared blood circulation. LP DC chimerism was analyzed two weeks after initiation of parabiosis. Graph shows the % of donor parabiont-derived cells among SB LP DC subsets in a recipient parabiont. **C. Origin of LP DCs in DC-depleted mice**. Twelve h after DT administration, CD45.2$^+$ CD11c-DTR chimeric mice were injected i.v. with MDP, CDP or Ly6C^{hi} monocytes and analyzed as described in (A). **D. Tracing the origin of LP DCs in reporter mice**. Graphs show the % of eGFP$^+$ cells among SB LP DC subsets in LysM-Cre × Rosa26-stop^{flox}EGFP mice.

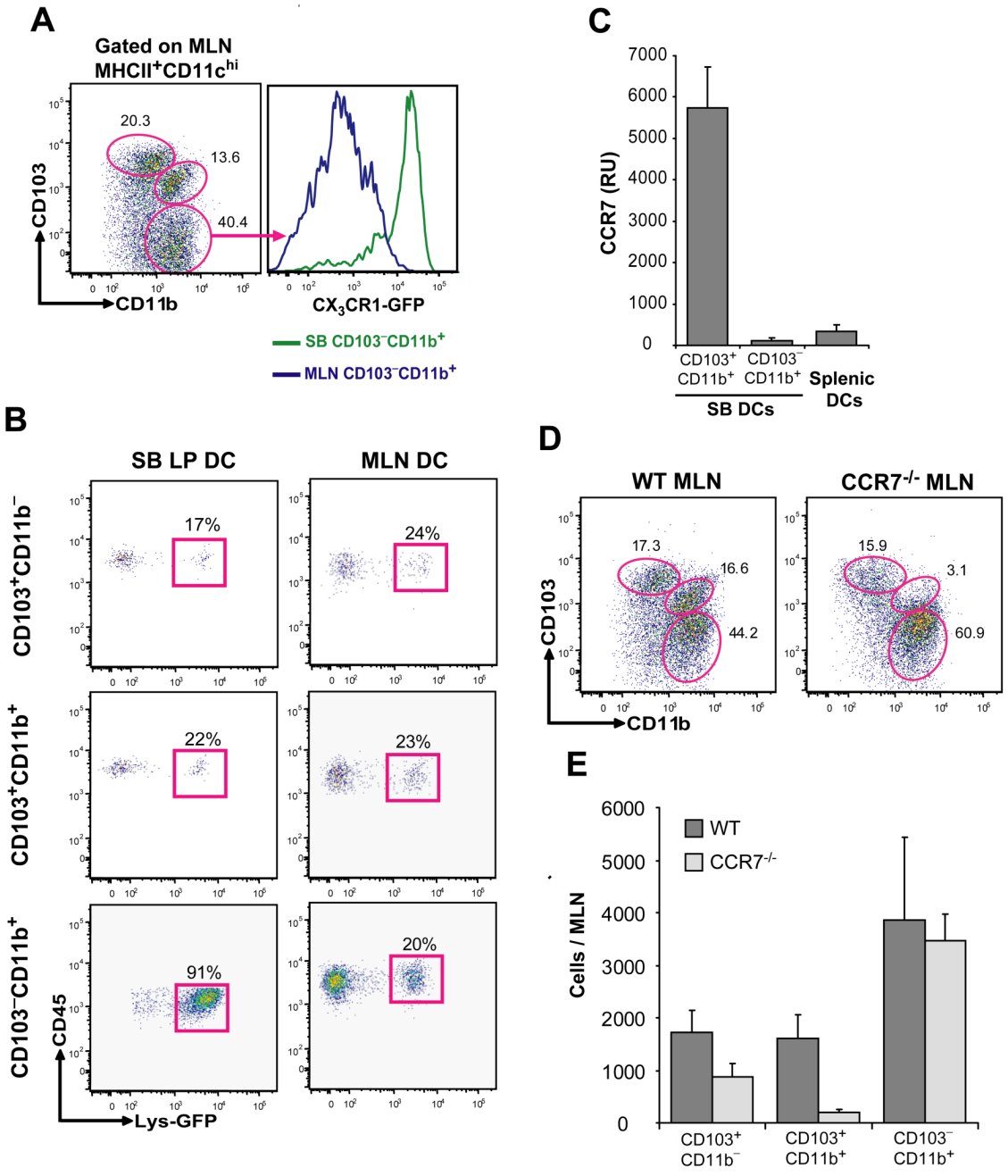

Figure 4. Migration of the LP DC subsets to the MLN in the steady state

A. Dot plots show the % of $CD103^{+}CD11b^{-}$, $CD103^{+}CD11b^{+}$ and $CD103^{-}CD11b^{+}$ DCs among $DAPI^{-}CD45^{+}MHCII^{hi}CD11c^{+}$ MLN DCs (left panel). Histograms show the CX3CR1 expression levels on gated $CD103^{-}CD11b^{+}$ MLN DCs compared to $CD103^{-}CD11b^{+}$ SB LP DCs isolated from $CX3CR1^{GFP/+}$ knock-in mice. **B**. Dot plots show the % $eGFP^{+}$ cells among total $CD103^{+}CD11b^{-}$, $CD103^{+}CD11b^{+}$ and $CD103^{-}CD11b^{+}$ SB LP DCs (left column) and MLN DCs (right column) in LysM-Cre × $Rosa26\text{-}stop^{flox}EGFP$ mice. Data represent one of 3 independent experiments. **C**. Bar graphs show CCR7 mRNA relative expression units (RU) in purified $CD103^{+}CD11b^{+}$ and $CD103^{-}CD11b^{+}$ SB LP DCs compared to purified splenic DCs from naive WT mice. Bar graph shows the mean ± SD of data from four independent cell

purifications tested in the same qPCR reaction. **D, E.** Dot plots and bar graph show the relative (D) and absolute (E) numbers of $CD103^{+}CD11b^{-}$, $CD103^{+}CD11b^{+}$ and $CD103^{-}CD11b^{+}$ MLN DCs in WT and $CCR7^{-/-}$ mice. Data represent the mean ± SD of 4 combined experiments.

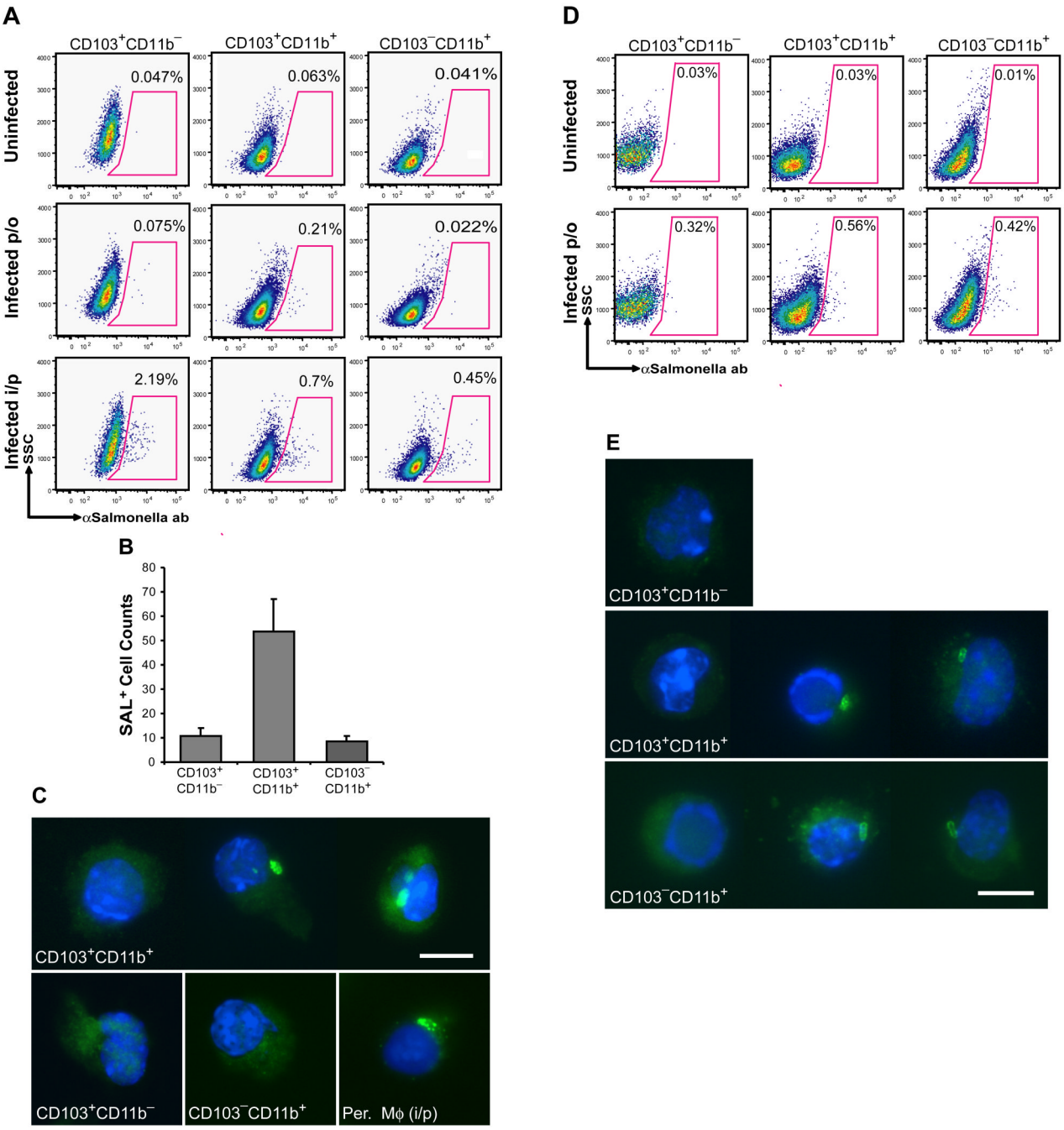

Figure 5. CD103$^+$CD11b$^+$ DCs are the first DCs to transport *Salmonella* Typhimurium to the MLN after oral infection

A–C. Mice were infected with *Salmonella* either orally (per os, p/o) or intraperitoneally (i/p). 18 h (i/p) or 24 h (p/o) post-infection, MLNs were collected and MLN single cell suspensions were stained for DC surface markers and intracellular *Salmonella* CSA and subjected to flow cytometry. **A**. Dot plots show the % of *Salmonella*$^+$ cells among each MLN DC subset after p/o or i/p infection compared to uninfected controls. **B**. Bar graph shows the absolute number of *Salmonella*$^+$ (SAL$^+$) cells among each MLN DC subset 24 h after oral infection. Data represent the mean ± SD of 3 independent experiments. **C**. Images show *S Salmonella* $^+$ cells in purified CD103$^+$CD11b$^+$ but not CD103$^+$CD11b$^−$ and CD103$^−$CD11b$^+$ MLN DC 24 h after

oral infection. Peritoneal macrophages (Per. Mφ) isolated 4 h after i/p infection, were used as a positive control. Magnification 600x. Scale bar 10 nm. **D–E**. 24 h after oral infection with *Salmonella*, SB were isolated and stained for DC surface markers and intracellular *Salmonella* antigens and analyzed by flow cytometry. **D**. Dot plots show the % of *Salmonella*$^{+}$ cells among each LP SB DC subset after oral (per os, p/o) infection compared to uninfected controls. **E**. Images show *Salmonella*$^{+}$ cells among purified SB LP CD103^{+}CD11b^{+} and CD103^{-} CD11b^{+} but not CD103^{+}CD11b^{-} DCs after oral infection. Magnification 600x. Scale bar 10 nm.

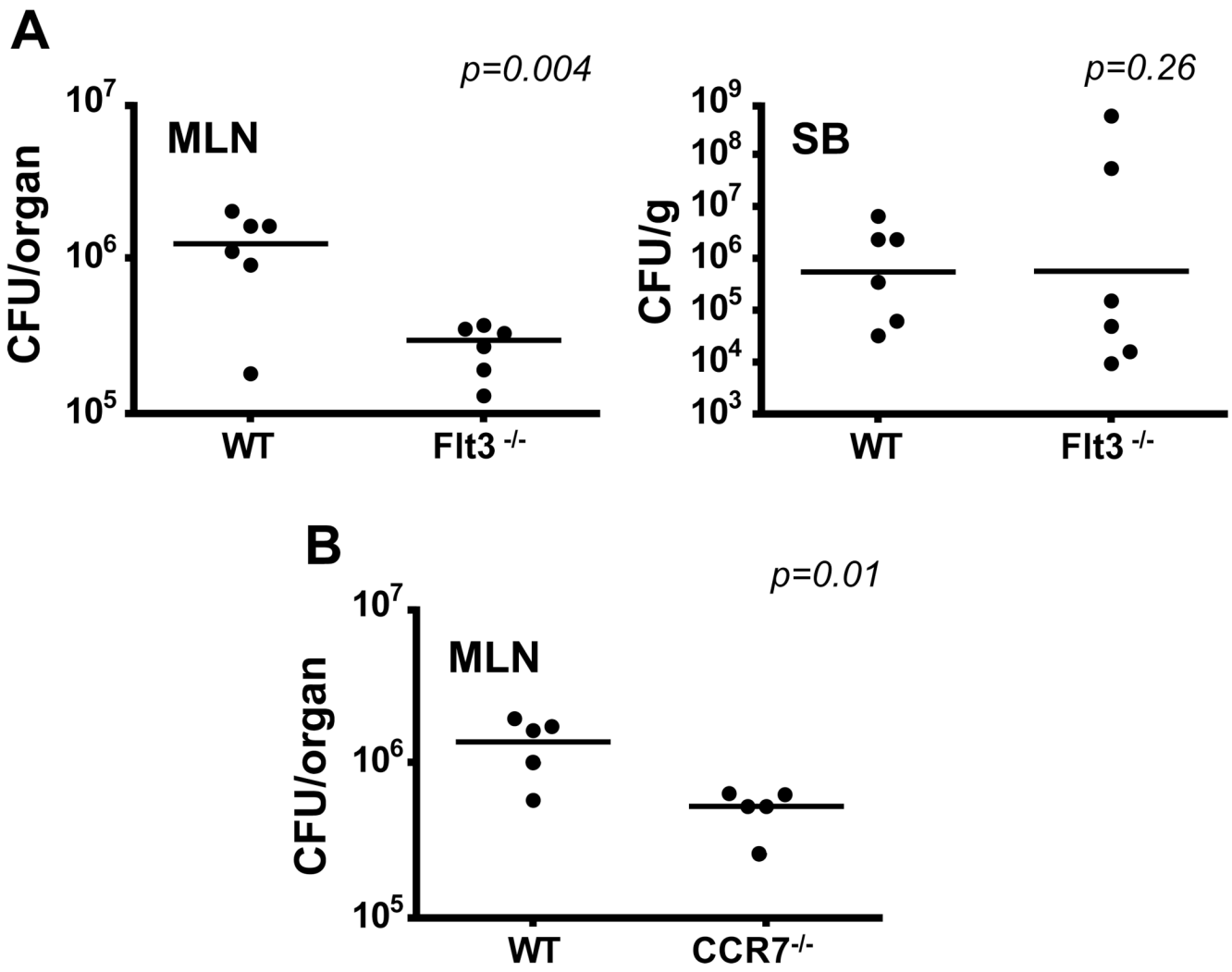

Figure 6. Transport of *Salmonella* Typhimurium to the MLN is impaired in Flt3$^{-/-}$ mice

A. Graphs show the numbers of *Salmonella* colony forming units (CFU) recovered from the homogenized terminal SB and total MLN of WT and Flt3$^{-/-}$ mice 2 days after oral *Salmonella* infection. Data represent the results of 3 independent experiments. **B**. Graphs show *Salmonella* CFU recovered from the homogenized total MLN of WT and CCR7$^{-/-}$ mice 2 days after oral *Salmonella* infection. Data represent the results of 3 independent experiments.